ISSN 0021-3640, JETP Letters, 2022, Vol. 115, No. 2, pp. 93–97. © The Author(s), 2022. This article is an open access publication, corrected publication 2022.
Russian Text © The Author(s), 2022, published in Pis'ma v Zhurnal Eksperimental'noi i Teoreticheskoi Fiziki, 2022, Vol. 115, No. 2, pp. 103–107.

CONDENSED MATTER

Theoretical Study of the Electronic and Transport Properties of Lateral 2D–1D–2D Graphene–CNT–Graphene Structures

B. Yu. Valeev[a, b, *], A. N. Toksumakov[a], D. G. Kvashnin[a, b], and L. A. Chernozatonskii[b, c]

[a] *Moscow Institute of Physics and Technology (National Research University), Dolgoprudnyi, Moscow region, 141701 Russia*

[b] *Emanuel Institute of Biochemical Physics, Russian Academy of Sciences, Moscow, 119334 Russia*

[c] *Scientific School on Chemistry and Technology of Polymer Materials, Plekhanov Russian University of Economics, Moscow, 117997 Russia*

**e-mail: bulat_valeev@phystech.edu*

Received November 15, 2021; revised November 25, 2021; accepted November 25, 2021

The electronic and transport properties of new hybrid 2D–1D–2D structures of carbon atoms, which are graphene sheets continuously connected through a fragment of a single-layer carbon nanotube, frequently observed experimentally, are theoretically studied. The evolution of the electronic properties of such systems with "zigzag" carbon nanotubes of various diameters with chirality indices (14, 0), (15, 0), (16, 0), and (18, 0) is studied using the tight coupling method within electron density functional theory. The calculation of the transmission coefficient demonstrates a strong nonlinearity in the behavior of the transport properties of these structures near the Fermi energy as a function of the diameter of carbon nanotubes, which explains discrepancies in the previously obtained experimental data.

DOI: 10.1134/S0021364022020114

INTRODUCTION

The fabrication of graphene [1] stimulated great interest in the study of the properties of two-dimensional structures with a thickness of one atom. As known, carbon nanotubes (CNTs) and their composites are still in the focus of attention because of their unique electronic properties, which are due to the one-dimensional nature of the material [2]. In particular, nanotubes are the smallest possible systems that can be used for efficient electron transport and therefore are of critical importance for the functioning of nanodevices.

Since it is difficult to use graphene as an element of semiconductor electronics because of its semimetallic band structure, possible ways to create a band gap in graphene-like structures while maintaining a high mobility of charge carriers in them were proposed. Among the most successful are the following: functionalization of graphenes (their hydrogenation [3], fluorination [4], oxidation [5]) and fabrication of graphene nanoribbons using electron lithography [6]. Separately, it should be noted that graphene can be present in the composition of hybrid carbon nanostructures, which are a combination of compounds from structures of different curvatures and dimensions, where carbon atoms are in sp^2 hybridization. Semiconducting CNTs, which are cylindrical carbon networks with certain chirality indices, which allows using them as filters for the passage of electrons with a certain energy, can serve as such components. Thus, the synthesis and creation of lateral devices based on graphene–CNT structures can become one of the promising directions for the development of post-silicon quasi-two-dimensional electronics because of the possibility of manufacturing a structure consisting entirely of carbon.

Note that recent successful experiments on the fabrication of graphene nanochannels by laser ablation [7, 8] reveal a new approach to the formation of graphene-based hybrid structures, which are of interest for planar nanoelectronics. Measurements of the electrical properties of the fabricated nanochannels demonstrate a nonlinear behavior of current–voltage characteristics (CVCs) when the resistance exceeds 20 kΩ, which indicates the presence of tunneling effects [9]. In addition, in an experimental study [10] of a narrow graphene island formed between two parts of graphene, the ballistic transfer and quantized conductivity of Dirac fermions were discovered. Consequently, nanochannels can be fabricated from a graphene ribbon by lithography. The mentioned experimental studies indicate the possibility of practical implementation of new hybrid structures, the electronic properties of which can be tuned by changing the geometric dimensions of the parts of such a system. Previously, studies of the mechanical properties [11], thermal conductivity [12], and electromagnetic

properties of similar nano-objects [13] were carried out.

It is well known that single-walled carbon nanotubes have high tensile strength and tensile modulus that are an order of magnitude higher than the respective characteristics of conventional carbon fibers [14, 15]. It was also demonstrated that the covalent bonding of one-dimensional (1D) structures (CNTs) with two-dimensional (2D) structures (graphene) can lead to the transfer of unique properties of CNTs to three-dimensional (3D) hybrid structures [16].

In this work, the electronic and transport properties of new lateral graphene–CNT–graphene systems, which were proposed on the basis of the available experimental data, are studied using the tight binding method. The features of the electron transmission spectra of such hybrid structures are studied and the dependence of the transport properties on the diameter of the CNTs covalently bonded to the edges of graphene sheets is described in detail.

CALCULATION METHODS

The atomic structure and the electronic and transport properties of the proposed graphene–CNT–graphene hybrid structures were studied using the self-consistent charge density functional tight binding (SCC-DFTB) approach [17, 18]. This method is widely used to describe the structural, electronic, and transport properties of carbon-based compounds containing a large number of atoms in the unit cell (more than 10^3). Geometrically restricted systems were processed using the supercell scheme allowing at least a 20-Å vacuum gap between them in the z direction, making intermolecular interactions negligible. The geometry of the selected structures was optimized until the change in the total energy became less than 10^{-4} eV and the forces acting on each atom became less than 10^{-3} eV/Å. The lattice parameters of the considered two-dimensional rectangular cell were 62.77 Å in the armchair direction and 61.52 Å in the zigzag direction.

These structures contained 702, 726, 742, and 782 carbon atoms and included sections of (14, 0), (15, 0), (16, 0), and (18, 0) CNTs, respectively, located between identical-size graphene electrodes. The DFTB+ program was used to model and evaluate the transport properties of systems in which ballistic transport occurs. This approach, based on the formalism of nonequilibrium Green's functions, allows the calculation of the electronic and transport properties of low-dimensional systems such as graphene nanoribbons in contact with two electrodes with different electrochemical potentials. In this case, graphene electrodes were used; therefore, their chemical potentials were the same as that of the interelectrode material. Each electrode used in transport calculations contained 92 carbon atoms. The electron transmission coefficients (T) through the considered structures were calculated using the retarded Green's function as follows [19]:

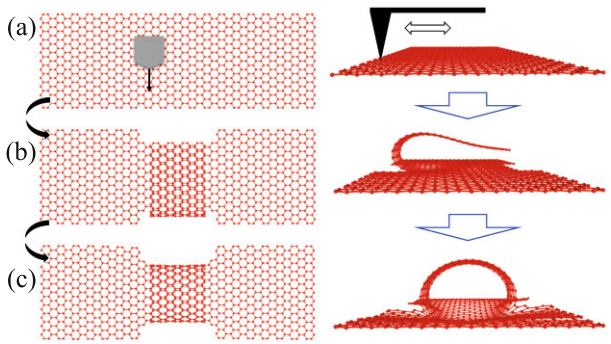

Fig. 1. (Color online) (a) Atomic structure of the considered cell of the original graphene sheet, (b) region of folded graphene between two graphene islands, and (c) connected edges of folded graphene, resulting in the formation of the (18, 0) carbon nanotube between two parts of graphene after optimization of the geometry.

$$\bar{T}_{RL}(E) = \mathrm{Tr}[\Gamma_R G^A \Gamma_L G^R].$$

Here, G^R is the retarded Green's function calculated only for the scattering region using the Hamiltonian of this region; $G^A = [G^R]^+$ is the advanced Green's function, where the superscript + stands for Hermitian conjugation; and Γ_R and Γ_L are the transfer matrices of the right and left electrodes, respectively, which are expressed as the imaginary part of the self-energies.

RESULTS AND DISCUSSION

One of the methods for obtaining various carbon nanostructures is based on laser ablation [8], which results in the evaporation of some carbon atoms in the selected region. Figure 1 demonstrates the atomic structures at the main stages of the proposed formation process. The cut graphene ribbon shown in the middle of the figure will tend to bend because of the low bending modulus of graphene [20], which contributes to sheet folding. The presence of dangling bonds at the edges of the graphene fragment can lead to the formation of a bond with another part of the fragment and the formation of a single-layer "zigzag" CNT between two graphene islands. This process of formation of the CNT from the folding of graphene pieces is well studied experimentally [21–23]. The resulting structure is a hybrid graphene–CNT–graphene structure. The ribbon length can be controlled by controlling laser pulses [9]; therefore, the diameter of the CNT can also be controlled. As will be shown below, a slight change in the diameter of a nanotube leads to a sharp change in the electronic properties of both the nanotube and the system itself.

In the study of transport properties, a graphene nanoribbon with armchair edges denoted as 23AGNR

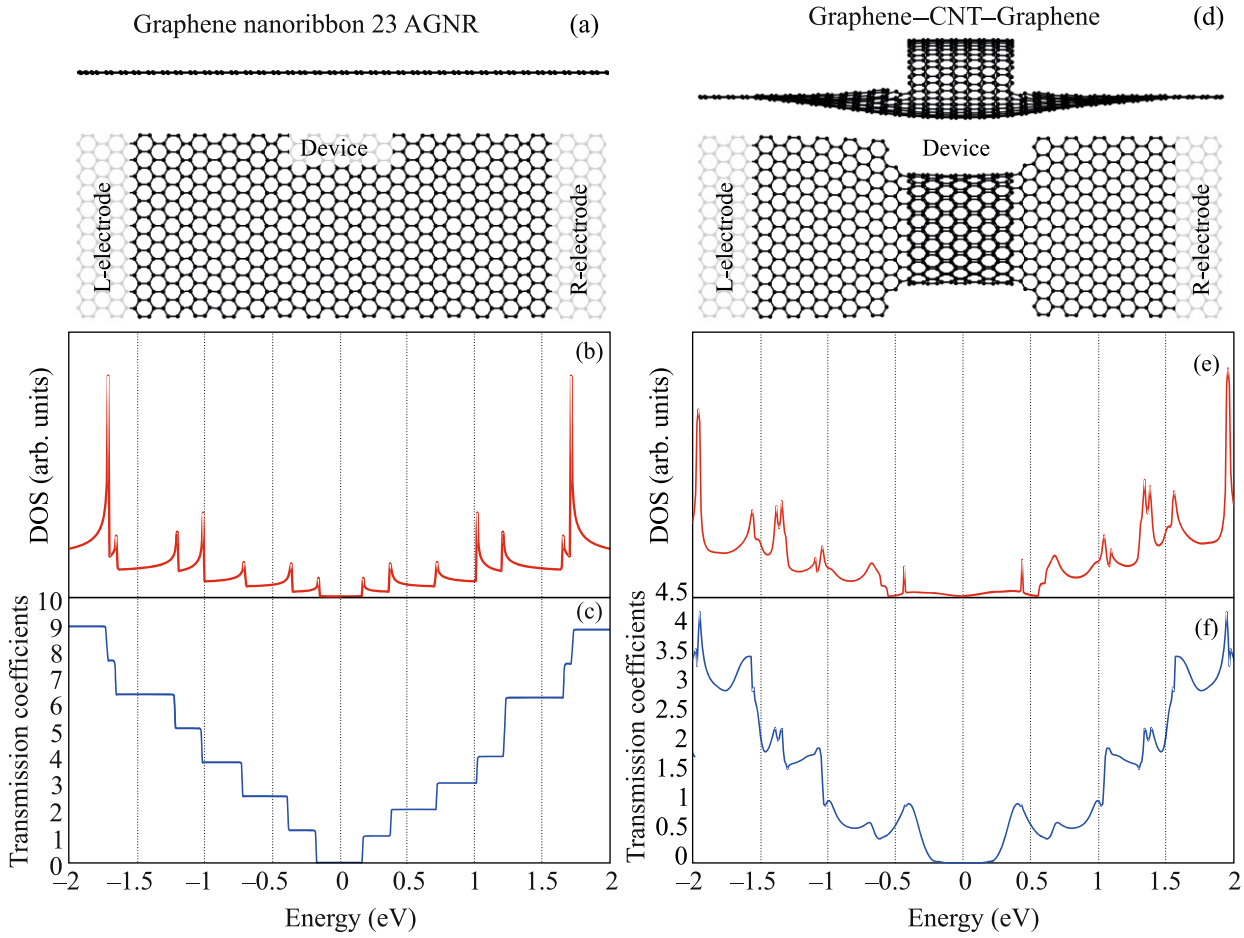

Fig. 2. (Color online) (a) Model of a graphene nanoribbon with the L and R electrodes, and Device regions selected for transport calculations, (b) graphene–(18, 0) carbon nanotube–graphene hybrid structure with the L and R electrodes, and Device regions, (c) density of electronic states, (d) density of states (DOS) for the graphene–carbon nanotube–graphene structure, (e) transmission coefficients, and (f) transmission coefficients. The energy is measured from the Fermi level.

(Armchair Graphene NanoRibbon), the atomic structure of which is demonstrated in Fig. 2a, was considered as a comparison device. The regions considered as the L and R electrodes correspond to the contact points, and the 2-nm-long section of the CNT channel is comparable with the corresponding sections in the devices from [10]. The same scheme was applied to calculate transmission coefficients for the graphene–CNT–graphene hybrid structure demonstrated in Fig. 2d, where the device was composed of two 23AGNR regions connected to each other by the 2-nm-long (18, 0) CNT. The calculated density of states for the 23AGNR demonstrates pronounced Van Hove singularities [24] and a narrow band gap of 0.4 eV (Fig. 2b), which is in good agreement with the published data [25]. The energy dependence of the transmission coefficient shown in Fig. 2c is a step function. Figures 2b and 2c demonstrate mirror symmetry with respect to the Fermi energy caused by the symmetry of the nanodevice with respect to its contacts. The density of states for the graphene–(18, 0) CNT–graphene structure is also symmetric, but with a slight distortion caused by the presence of dangling bonds at the edges of the nanotube (Fig. 2e). Such a device has a band gap of about 0.5 eV, which is larger than a value of 0.3 eV in the case of a single 23AGNR region (Fig. 2b). The transmission coefficient near the Fermi energy shows maximum values at energies of –0.4 and 0.4 eV (Fig. 2f).

The dependence of transmission coefficients on the diameter of CNTs was studied to evaluate the effect of geometric parameters of CNTs in graphene–CNT–graphene hybrid systems. Carbon nanotubes with the indices (16, 0), (15, 0), and (14, 0) were also considered. The atomic structure of the proposed devices with CNTs of different diameters and the basic calculation scheme are similar to those demonstrated in Fig. 2d, and the dependences of the transmission coefficients are demonstrated in Fig. 3.

It can be seen that a decrease in the nanotube diameter from (18, 0) to (16, 0) leads to a shift in the maxima of the transmission coefficients. In the case of

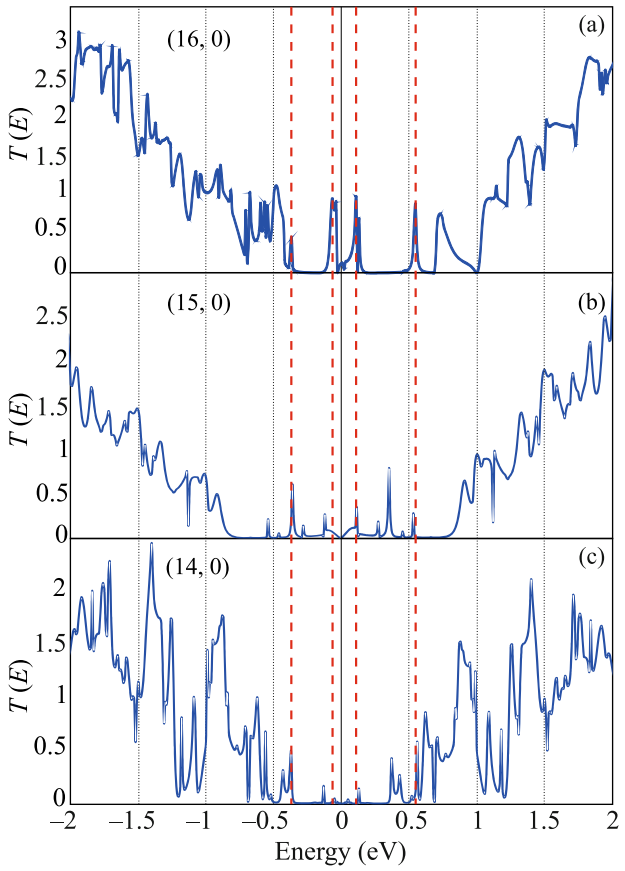

Fig. 3. (Color online) Transmission coefficient versus the energy for graphene–carbon nanotube–graphene structures with the (a) (16, 0), (b) (15, 0), and (c) (14, 0) carbon nanotubes. The red dotted lines (for clarity) indicate the maximum values of the transmission coefficient for the (16, 0) carbon nanotube near the Fermi energy.

the (16, 0) CNT, the maxima are observed at energies of –0.05 and 0.1 eV (while the maxima for the (18, 0) CNT were observed at energies of –0.4 and 0.4 eV). A further decrease in the diameter of the CNT (Fig. 3) in the charge carrier scattering region leads to the formation of additional maxima of the transmission coefficient. For example, a new maximum for the (15, 0) CNT (compared to the (16.0) CNT) is observed at energies of –0.25 and 0.25 eV. An analogous maximum also appeared for the smallest of the considered scattering regions of the (14, 0) CNT. The new maximum of the transmission coefficient for the (15, 0) CNT and (14, 0) CNT is observed at energies from 0.3 to 0.45 eV.

Thus, the resonant behavior of the current–voltage characteristics in the considered graphene–CNT–graphene systems is observed in a wider range of applied electrical voltages than in the nanoribbon on the basis of which they were designed [26]. It should be expected that the transport properties in these nanodevices will also respond to the excitation of carriers by light at resonant frequencies (from the valence band to the conduction band), as occurs in perforated bigraphene structures [27]. In addition, the features of the atomic geometry of nanostructures can lead to the appearance of nonlinear effects, by analogy with two-band structures [28], nanostructures on perforated two-layer graphene nanoribbons, and transition metal dichalcogenides [26, 29].

CONCLUSIONS

In this work, new lateral graphene–CNT–graphene nanostructures based on the available experimental observations have been proposed [16]. Using the SCC-DFTB approximation, we have studied the influence of the formation of CNTs in the central region of graphene on the electronic and transport characteristics of this type of systems. The data obtained demonstrate the formation of maxima of the transmission coefficient depending on the diameter of the CNT, which corresponds to the formation of new conducting channels in the proposed graphene–CNT–graphene hybrid structures. The simulation results explain the inhomogeneity of the conductive properties of graphene nanostructures obtained by electron lithography and laser ablation and show the promise of using the studied resonant nonlinearity in nanodevices based on the considered lateral graphene–CNT–graphene structures.

ACKNOWLEDGMENTS

We are grateful to Prof. Filipp Lambin, Dr. Sci. (Phys.–Math.) Aleksandr Gennad'evich Kvashnin, and Zakhar Ivanovich Popov for stimulating discussion of the work.

FUNDING

The work was supported by the Ministry of Science and Higher Education of the Russian Federation (project no. 01201253304). Part of the calculations were performed using the resources of the Joint Supercomputer Center, Russian Academy of Sciences (JSCC RAS).

CONFLICT OF INTEREST

The authors declare that they have no conflicts of interest.

REFERENCES

1. K. S. Novoselov, D. Jiang, F. Schedin, T. J. Booth, V. V. Khotkevich, S. V. Morozov, and A. K. Geim, Proc. Natl. Acad. Sci. U. S. A. **102**, 10451 (2005).
2. S. Iijima, Nature (London, U.K.) **354**, 56 (1991).
3. D. C. Elias, R. R. Nair, T. M. G. Mohiuddin, S. V. Morozov, P. Blake, M. P. Halsall, A. C. Ferrari, D. W. Boukhvalov, M. I. Katsnelson, A. K. Geim, and K. S. Novoselov, Science (Washington, DC, U. S.) **323**, 610 (2009).
4. R. R. Nair, W. Ren, R. Jalil, I. Riaz, V. G. Kravets, L. Britnell, P. Blake, F. Schedin, A. S. Mayorov, S. Yuan, M. I. Katsnelson, H.-M. Cheng, W. Strupinski, L. G. Bulusheva, A. A. Okotrub, and I. V. Grigorieva, Small **6**, 2877 (2010).
5. C. Gómez-Navarro, J. C. Meyer, R. S. Sundaram, A. Chuvilin, S. Kurasch, M. Burghard, K. Kern, and U. Kaiser, Nano Lett. **10**, 1144 (2010).
6. L. Tapasztó, G. Dobrik, P. Lambin, and L. P. Biró, Nat. Nanotechnol. **3**, 397 (2008).
7. K. Xia, H. Zhan, and Y. Gu, Proc. IUTAM **21**, 94 (2017).
8. https://www.diva-portal.org/smash/get/diva2:1529856/FULLTEXT01.pdf.
9. I. Silvestre, A. W. Barnard, S. P. Roberts, P. L. McEuen, and R. G. Lacerda, Appl. Phys. Lett. **106**, 153105 (2015).
10. B. Terrés, L. A. Chizhova, F. Libisch, J. Peiro, D. Jörger, S. Engels, A. Girschik, K. Watanabe, T. Taniguchi, S. V. Rotkin, J. Burgdörfer, and C. Stampfer, Nat. Commun. **7**, 11528 (2016).
11. A. S. Kolesnikova, I. V. Kirillova, G. A. Baregamyan, and L. Yu. Kossovich, Vestn. Samar. Tekh. Univ., Ser. Fiz.-Mat. Nauki **22**, 574 (2018).
12. Z. Yu, Y. Feng, D. Feng, and X. Zhang, Phys. Chem. Chem. Phys. **22**, 337 (2019).
13. J. Joseph, P. R. Munda, D. A. John, A. M. Sidpara, and J. Paul, Mater. Res. Express **6**, 085617 (2019).
14. R. Zhang, Q. Wen, W. Qian, D. S. Su, Q. Zhang, and F. Wei, Adv. Mater. **23**, 3387 (2011).
15. D. Tasis, N. Tagmatarchis, A. Bianco, and M. Prato, Chem. Rev. **106**, 1105 (2006).
16. Y. Zhu, L. Li, C. Zhang, G. Casillas, Z. Sun, Z. Yan, G. Ruan, Z. Peng, A.-R. O. Raji, C. Kittrell, R. H. Hauge, and J. M. Tour, Nat. Commun. **3**, 1225 (2012).
17. M. Elstner, D. Porezag, G. Jungnickel, J. Elsner, M. Haugk, T. Frauenheim, S. Suhai, and G. Seifert, Phys. Rev. B **58**, 7260 (1998).
18. A. Pecchia and A. D. Carlo, Rep. Prog. Phys. **67**, 1497 (2004).
19. D. S. Fisher and P. A. Lee, Phys. Rev. B **23**, 6851 (1981).
20. K. N. Kudin, G. E. Scuseria, and B. I. Yakobson, Phys. Rev. B **64**, 10 (2001).
21. X. Xie, L. Ju, X. Feng, Y. Sun, R. Zhou, K. Liu, S. Fan, Q. Li, and K. Jiang, Nano Lett. **9**, 2565 (2009).
22. J.-W. Liu, J. Xu, Y. Ni, F.-J. Fan, C.-L. Zhang, and S.-H. Yu, ACS Nano **6**, 4500 (2012).
23. M. Quintana, M. Grzelczak, K. Spyrou, M. Calvaresi, S. Bals, B. Kooi, G. van Tendeloo, P. Rudolf, F. Zerbetto, and M. Prato, J. Am. Chem. Soc. **134**, 13310 (2012).
24. G. Li, A. Luican, J. M. B. Lopes dos Santos, A. H. C. Neto, A. Reina, J. Kong, and E. Y. Andrei, Nat. Phys. **6**, 109 (2010).
25. M. Y. Han, B. Özyilmaz, Y. Zhang, and P. Kim, Phys. Rev. Lett. **98**, 206805 (2007).
26. V. A. Demin, D. G. Kvashnin, P. Vancso, G. Mark, and L. A. Chernozatonskii, JETP Lett. **112**, 305 (2020).
27. L. A. Chernozatonskii, A. A. Artyukh, A. G. Kvashnin, and D. G. Kvashnin, Appl. Mater. Interfaces **12**, 55189 (2020).
28. I. L. Drichko, I. Yu. Smirnov, A. K. Bakarov, A. A. Bykov, A. A. Dmitriev, and Yu. M. Gal'perin, JETP Lett. **112**, 45 (2020).
29. M. M. Glazov and E. L. Ivchenko, JETP Lett. **113**, 7 (2021).

Translated by R. Bando